

# Object extraction at nano-surface images

A. Nedzved<sup>1)</sup>, O. Nedzved<sup>2)</sup>, S. Ablameyko<sup>1)</sup>, S. Uchida<sup>3)</sup>

1) United Institute of Informatics Problems of the National Academy of Sciences, Belarus. e-mail: abl@newman.bas-net.by

2) Belarusian State Medical University, Belarus, e-mail: olga\_nedzved@tut.by,

3) IS Dept, Kyushu University, Japan. e-mail: uchida@is.kyushu-u.ac.jp

## 1. INTRODUCTION

Recently with fast development of nanotechnologies, atomic force microscopy (AFM) are started widely used. They allow determining the sizes of structural elements and mechanical properties of objects at nano-surfaces [1]. The individual atoms, molecules and large macro-associations are considered in studying the characteristics of nano-scale objects.

However, further image analysis methods should be used to extract objects and their characteristics. This is quite difficult task because nano-surface images have many specifics. There are attempts to process such type or similar images [2-5]. However, each concrete case should be considered in details. We considered processing magneto-optical images in our papers [6-7]. This study continues analysis of magneto-optical images moving to nano-surface images.

In the paper, the processing scheme, methods of constructing finite element models of nano-samples of AFM images, setting rules of the boundary conditions for simulation of contact interaction are proposed. The results of computational experiments to determine the characteristics of image objects by means of the package LS-DYNA are presented.

## 2. SPECIFICS OF NANO-SURFACE IMAGES

The nano-surface objects can be represented as hemispheres. They are presented as rounded regions with increasing brightness toward the center on grayscale nano-images (Figure 1).

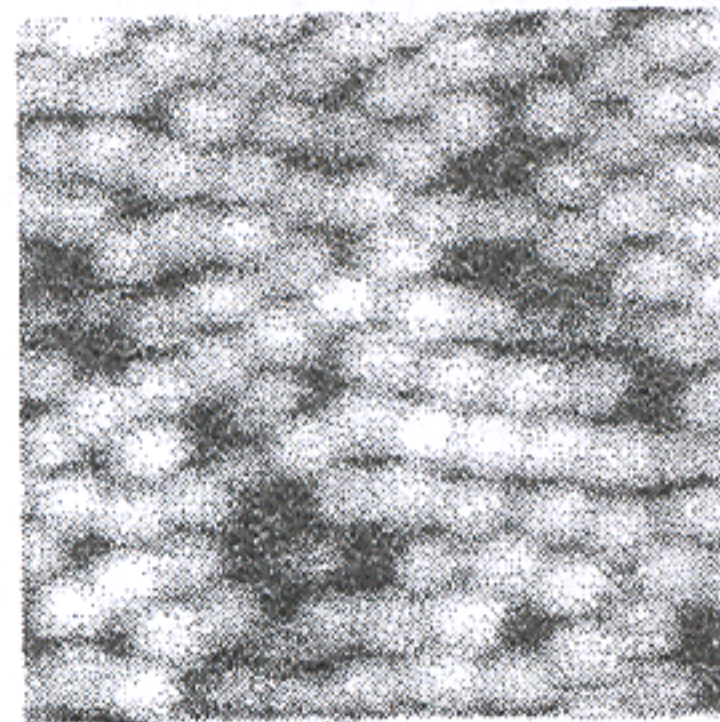


Fig. 1 – Grayscale image of nano-surface with spherical objects

The brightness profile of the original image horizontally is represented by a smooth line (Figure 2). A profile in the vertical direction has high contrast and small overshoots (Figure 3).

There is a heterogeneous geometric contrast on the image where the vertical changes component is much higher than horizontal component. This effect is related to the conditions of imaging. The process of constructing an image is based on scanning the surface of the cantilever. After scanning, at the image the duration of receipt of the adjacent vertical pixels is significantly higher than the

duration of receipt of horizontal pixels. The result is affected by a number of external interference: a geometric drift and the drift of brightness.

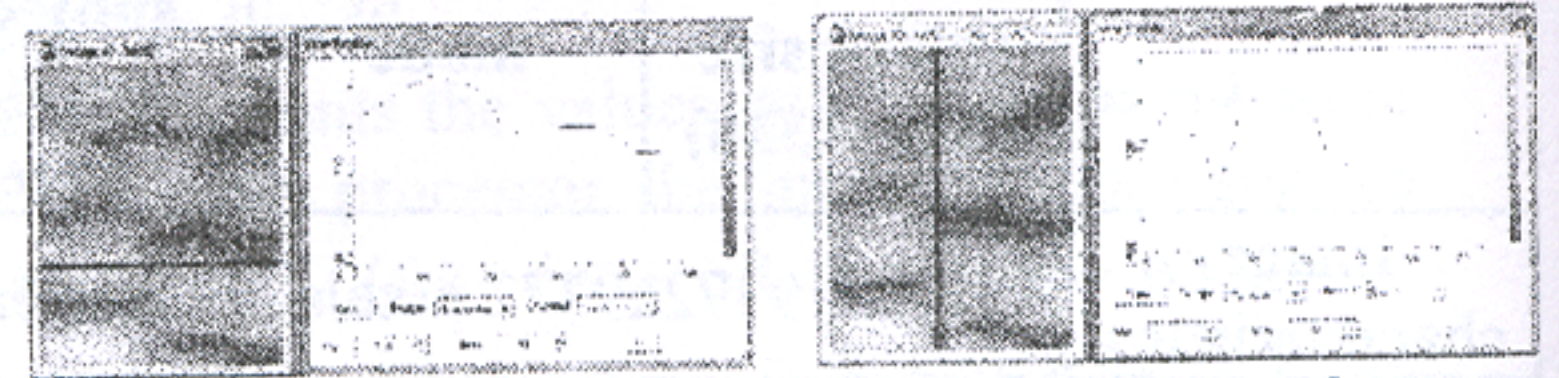


Fig. 2 – Brightness profile of horizontal and vertical direction

Also a cantilever has a certain inertia in the time of the horizontal scanning. This causes to the fact that the properties of light in each line receive the unique features. Such heterogeneity is reflected in the global brightness histogram (Figure 3). Histogram of the nano-surface is similar to a Gaussian distribution. But it has a lot of individual pulses that sharply differ from their neighbors. A removing or compensation for these defects is necessary because they affect the quality of image processing.

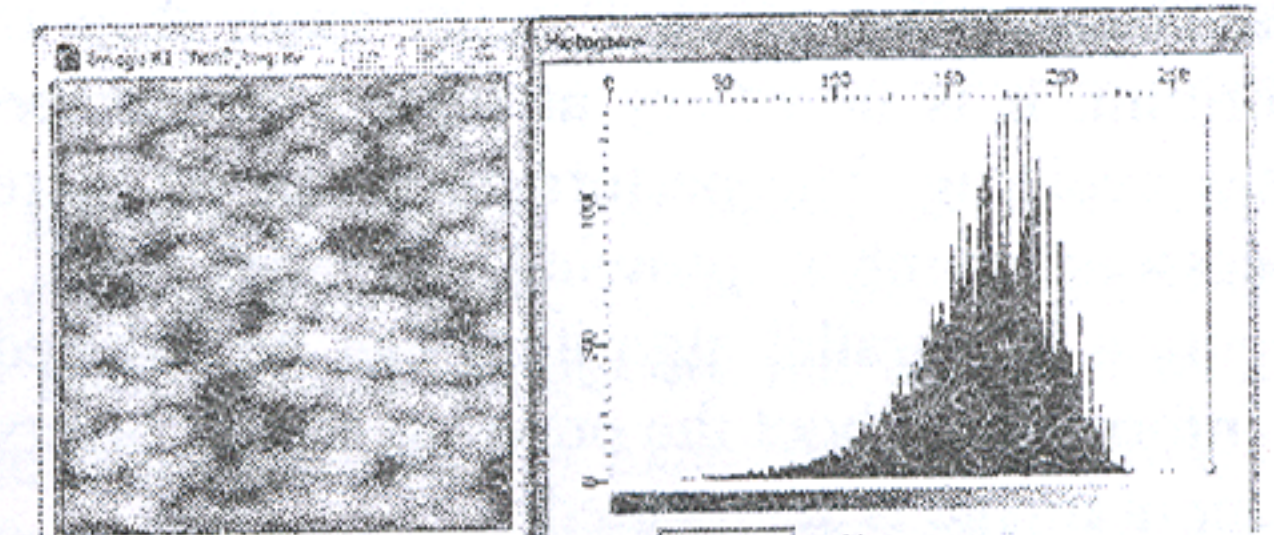


Fig. 3 – Histogram of the nano-surface image

## 3. CORRECTION OF LOCAL CONTRAST HETEROGENEITY

Geometric heterogeneity of the contrast in images obtained by atomic force microscopy is a serious problem which solution in the general case has not yet been found.

In this paper, we propose two approaches. The first one is to generate a possible background for the image, the second is based on the calculation of the characteristics of local contrast for vertical and horizontal lines. Both approaches are based on the assumption of symmetry of objects at the nano-surface.

In the first method, two background images are generated. One is created by repeated application of a simple averaging convolution with a large raster (for 256x256 image – bitmap 14x14):

$$I_{xy} = \frac{1}{2 \cdot n} \sum_{i=y-n}^{y+n} \sum_{j=x-n}^{x+n} I_{ij}$$

where  $I_{xy}$  – value of the pixel on the image with coordinates  $x, y$ ,  $n$  – the half-size of the raster convolution.

As a result of this transformation an image corresponding to dark backgrounds<sup>3)</sup> is obtained (Figure 5. b).

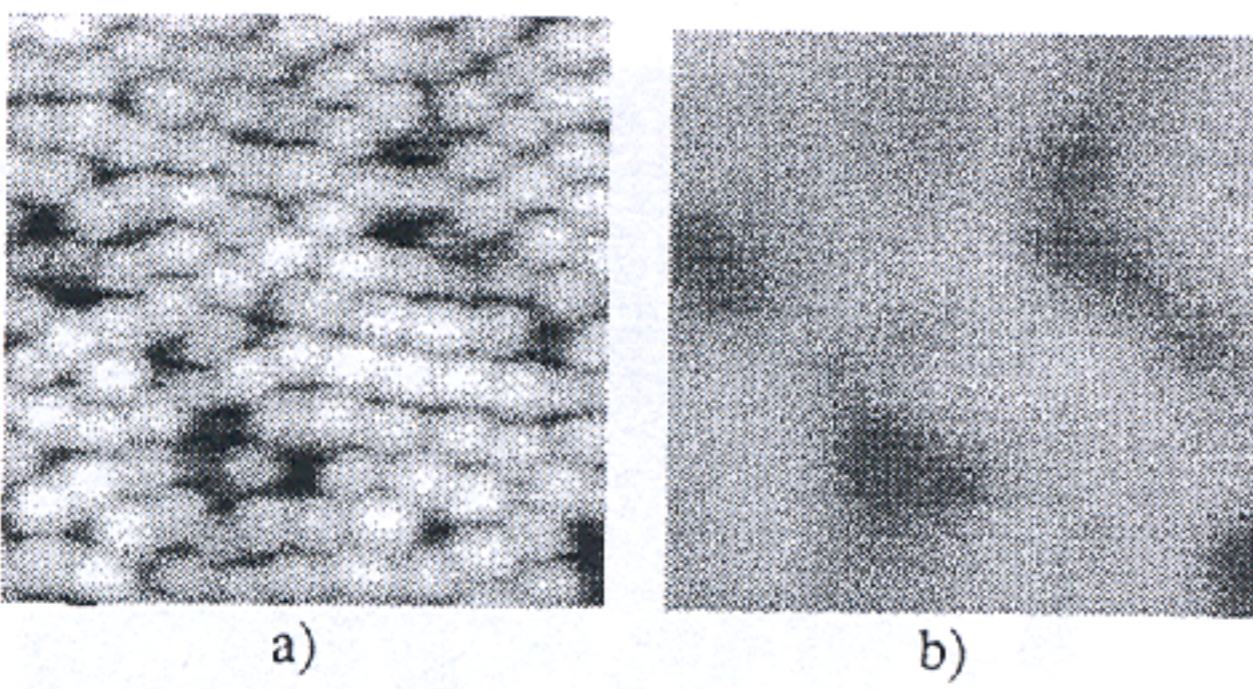


Fig. 5 – Image of nano-surface (a) and generated dark background (b)

A second background image corresponds to the maximum level, i.e. illumination of the image.

This image is generated by several iterations of grayscale image dilation with structuring element 5x5) (for an image 256x256 – 2 iterations).

Dilation of the set  $A$  by the structuring element  $B$  is defined as

$$A \oplus B = \left\{ z \mid \left( \hat{B} \right)_z \cap A \neq \emptyset \right\}$$

At the core of this relation is an operation of obtaining the central reflection of the set  $B$  respect to its origin of coordinates and displacement of the resulting set to the point  $z$ . In this case a dilation of  $A$  to  $B$  is the set of all such displacements, in which the sets  $B$  and  $A$  coincide. For grayscale pixel a shifting of boundaries occurs, i.e. a current pixel is assigned the value of its neighbors. The result is an image of merged objects (Figure 4).

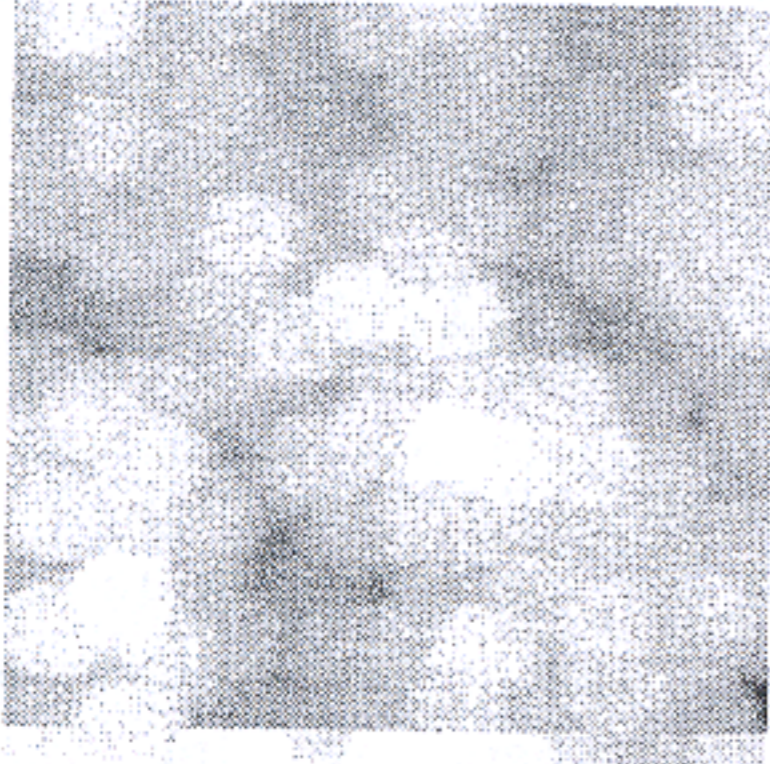


Fig. 4 – Background image of maximum brightness

With two limits for image brightness it is possible to determine approximately the local contrast of each point. It is roughly equal to the difference between limits. On the basis of these data, we can determine the change of contrast at each point. However, this operation is not effective. Based on the two background images we can perform the background correction. This operation compensates the shortcomings of spatial heterogeneity of contrast:

$$C_{x,y} = \frac{(I_{x,y} - B_{x,y}) \cdot (W_{max} - B_{x,y})}{(W_{x,y} - B_{x,y})}$$

where  $I_{x,y}$  – a brightness value pixel of the image with the magneto-optic component;  $B_{x,y}$  – a pixel value for image with a constant component;  $W_{x,y}$  – the pixel value for the image with the full saturation (illumination);  $W_{max}$  – the maximum brightness of the image at a saturation of brightness;  $C_{x,y}$  – a new brightness value of the pixel in the corrected image (Figure 6).

However the image contains horizontal lines and contrast of these lines is even increased. This defect is compensated by the median filtering which allows smoothing of the surface of the image.

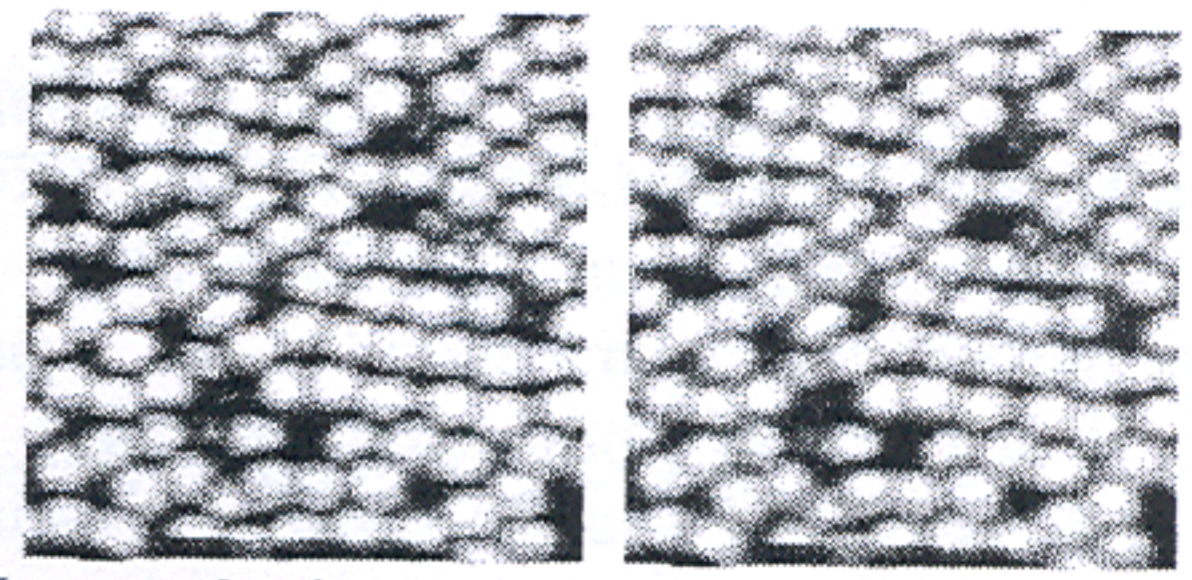


Fig. 6 – Image obtained after correction of the background (a) and after an additional median filtering (b)

The second method consists in the calculation of the local contrast. It consists in determining the numerical value of local contrast for each image line, its non-linear amplification, and recovery of the same line with the image brightness variations. It provides a local contrast amplification along the lines in comparison with the original image. The procedure for amplification of the local contrast consists of three main phases. It is used for each element of  $L(i, j)$  with coordinates  $(i, j)$  of the original image.

In practice the efficiency of the method is not sufficient for image processing if images contain small parts such as the gaps between objects. This occurs because the value of the local contrast is proportional to difference between the central element of the image and the surrounding background to the brightness. This formula includes the element values or their average values, which leads to an incomplete description of the texture of the local area. Statistical methods describe texture characteristics such as homogeneity, roughness and granularity most completely.

One of the most common methods for describing texture is to use moments of the histogram of the intensities of image elements. Let  $L$  – random variable, which defines a discrete image intensity,  $H(L(i, j))$  – the corresponding values of the histogram. It is known that the  $n$ -th moment of  $L(i, j)$  with respect to the average value is determined by

$$\mu_n(L) = \sum_{(i,j) \in W} (L(i, j) - \bar{L})^n H(L(i, j))$$

where  $\bar{L}$  is the average brightness of the elements of the local neighborhood of  $W$ .

From this expression it follows that  $\mu_0=1$  and  $\mu_1=0$ . The second moment corresponds to the dispersion  $\sigma^2(L)$  and is used to describe of the texture. He is also a measure of the intensity and contrast can be used to describe a uniform surface. As a result as a measure of contrast of textures is proposed to use the expression

$$C(i, j) = 1 - \frac{1}{1 + k\sigma^2(L)}$$

where  $\sigma^2(L)$  – dispersion in the neighborhood  $n \times m$ ,  $k=0,8$  – normalization factor.  $C(i, j)$  is equal to zero for the neighborhoods with a constant intensity and it is equal to one for large values of  $\sigma^2(L)$ . It is fully compliant with determination of the local contrast.

Thus the first phase of the proposed method requires to calculate the local contrast for each picture element as  $C(i, j)$ . Next the nonlinear transformation of the local contrast is carried out  $C(i, j)$ . Then the image is reconstructed by identifying a new brightness values of pixels of the lines  $L^*(i, j)$ . For this the expression is proposed:

$$L^*(i, j) = L(i, j) + \left( \frac{C^*(i, j) * n * m}{1 - C^*(i, j)} - \sum_{\forall(i, j) \in \mathbb{R}_2 - \mathbb{R}_1} (L(i, j) - L(i, j))^2 H(L(i, j)) \right)^{0.5}$$

This procedure is repeated for each element of each horizontal image line.

The proposed algorithm uses the statistical definition of local contrast. Due to this the homogeneity of texture, its "roughness" and granularity are taken into account (Figure 7).

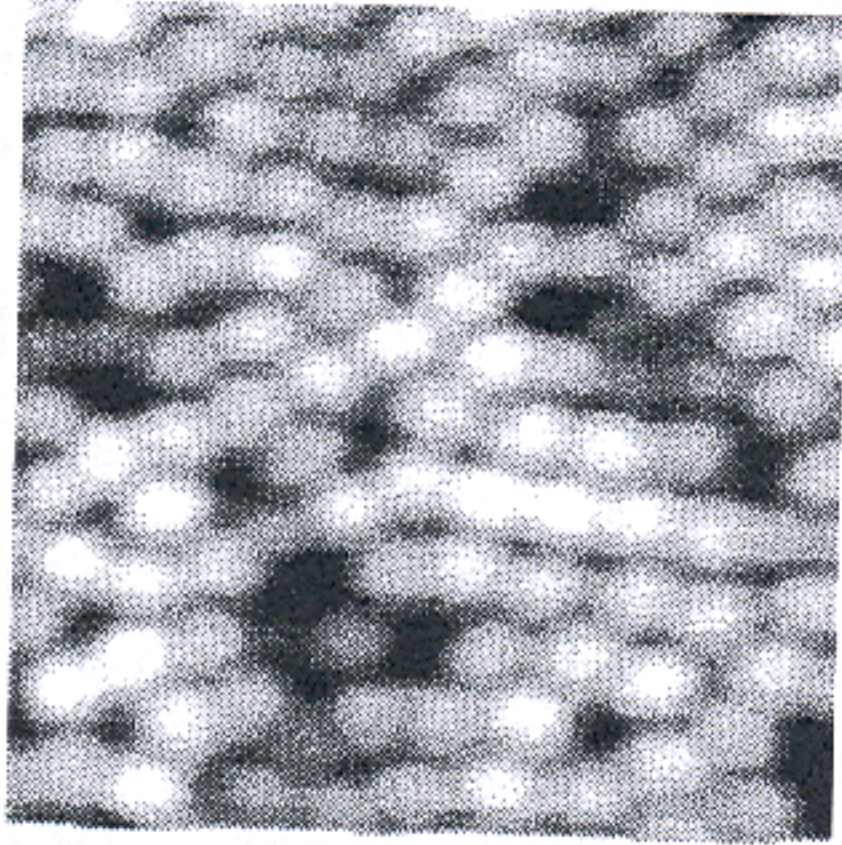


Fig. 7 – The result of the local correction of the contrast on the image of nano-surface

The experiment showed that the second method gives a clearer picture as a result, but the first method works three times faster.

#### 4. OBJECT EXTRACTION AT NANO-SURFACE IMAGES

Objects that form the surface are the basis for determination of its characteristics: size, shape, height and position. To determine these characteristics is it necessary to find applicable objects in the image.

The selection of objects can be carried out in different ways. We assume that the objects are presented as spheres that intersect. In this case they can be represented as a topological surface. Then it is possible to determine the position of cavities between them.

##### 4.1 WATERSHED-BASED IMAGE SEGMENTATION

Watershed algorithm is used for determining the boundary lines between objects. The resulting image is often divided into a large number of small areas (pools), most of which are not significant in solving the problem.

Lines of the watershed of the image are the boundaries that separate areas of this image. In the topographic representation of images, numerical values (such as gray levels) for every pixel serve as the height of this point. The main problem of this algorithm is over-segmentation, because all boundaries and noises are displayed in the gradient. Therefore the process of noise removal is necessary.

As a result the direct application of this algorithm to the image of nano-surface gives additional false objects (Figure 8).

Application of contrast correction before the noise filtering significantly improves the result (Figure 9).

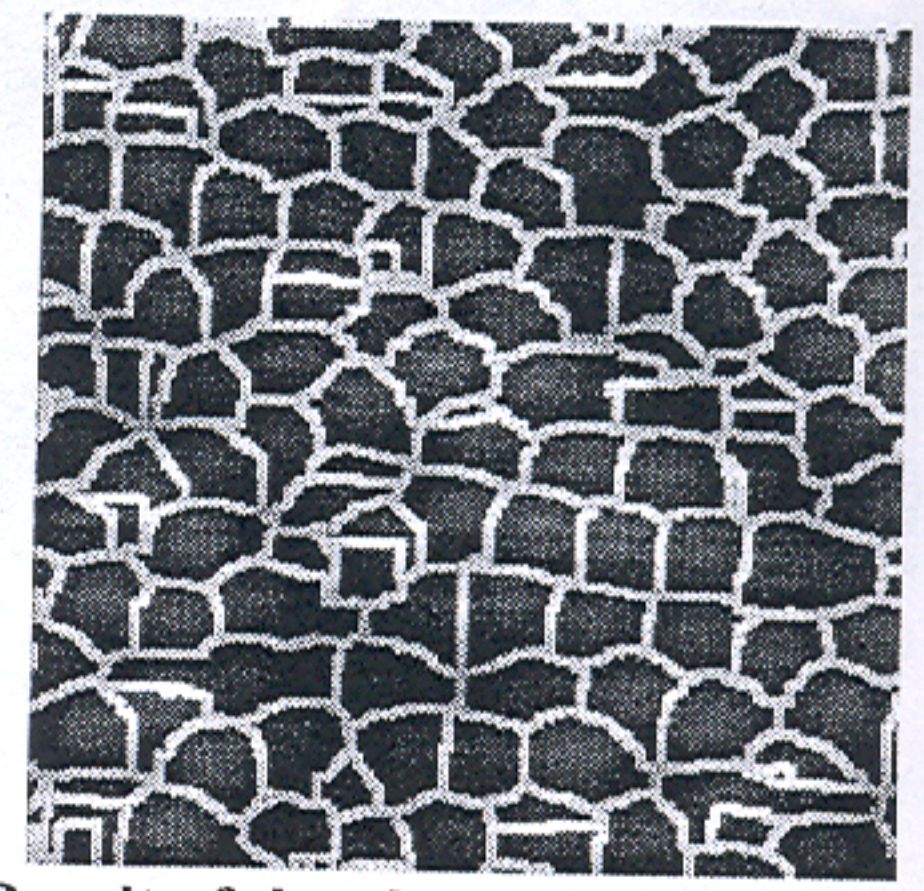


Fig. 8 – Result of the algorithm watershed applied directly to the image of nano-surface

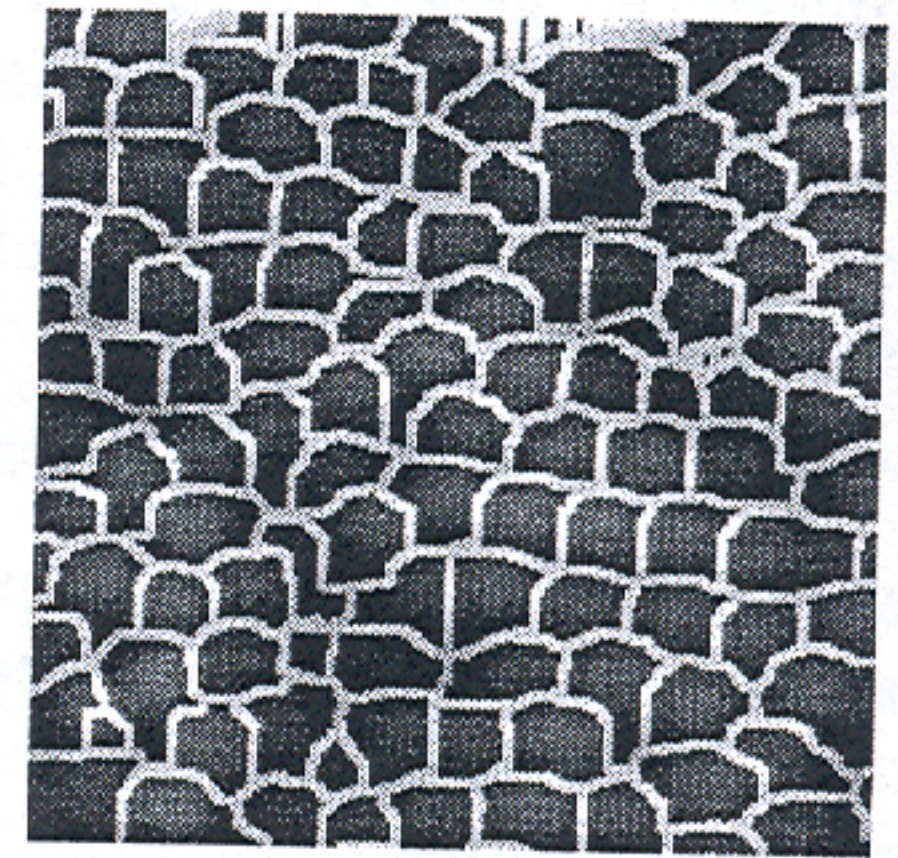


Fig. 9 – The result of watershed algorithm applied to image of the nano-surface after local contrast correction and a noise filtering

The algorithm allows obtaining the boundary of objects. However, the boundary lines are slightly chopped because a transformation uses urban metrics of computation of distances.

##### 4.2 OBJECT EXTRACTION AT SEGMENTED IMAGE

As mentioned above the objects in the image represent hemispheres but the image boundaries mainly composed of polygons. To solve this problem, a special algorithm for correcting the shape on the basis of mathematical morphology was developed.

The first step of algorithm is the the inversion of boundaries Then objects clasped to the edge are removed (Figure 10).

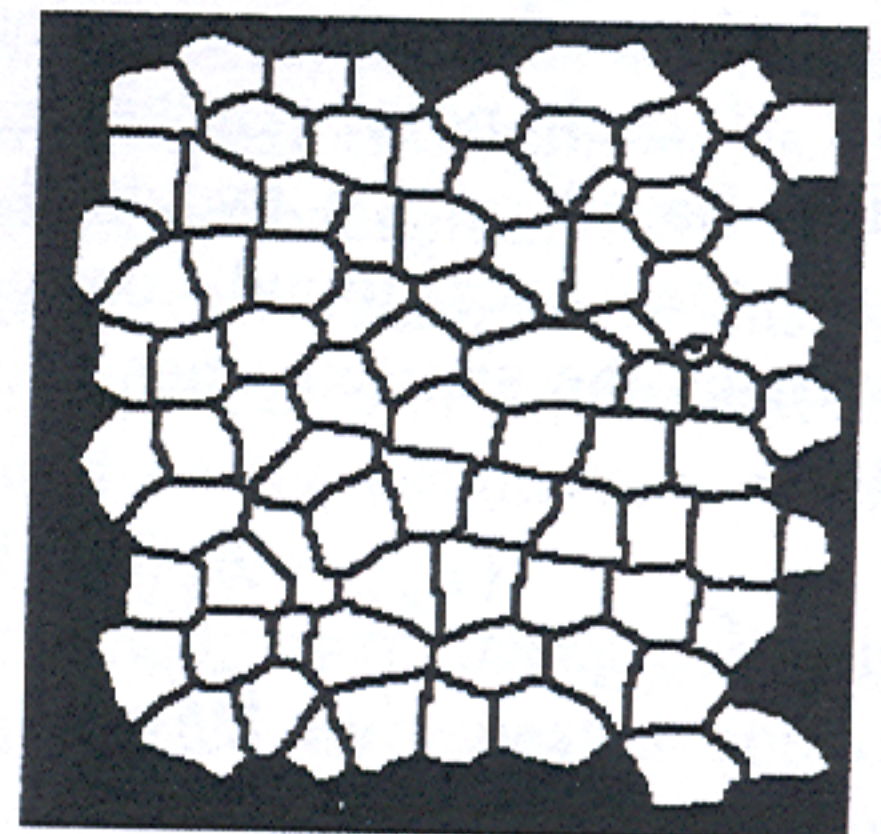


Fig. 10 – The result of removing of objects clasped to the edge

The image contains small objects that have emerged in the empty fields. They are removed by a noise filtering by area (Figure 11).

Then the correction of boundaries of objects by using morphological opening operation is performed (Figure 12).

In the result objects of nano-surface image are extracted. This algorithm has several advantages compared with the original method. It allows to extract objects and calculate the series of geometric and brightness

characteristics which can be used for a more complete description.

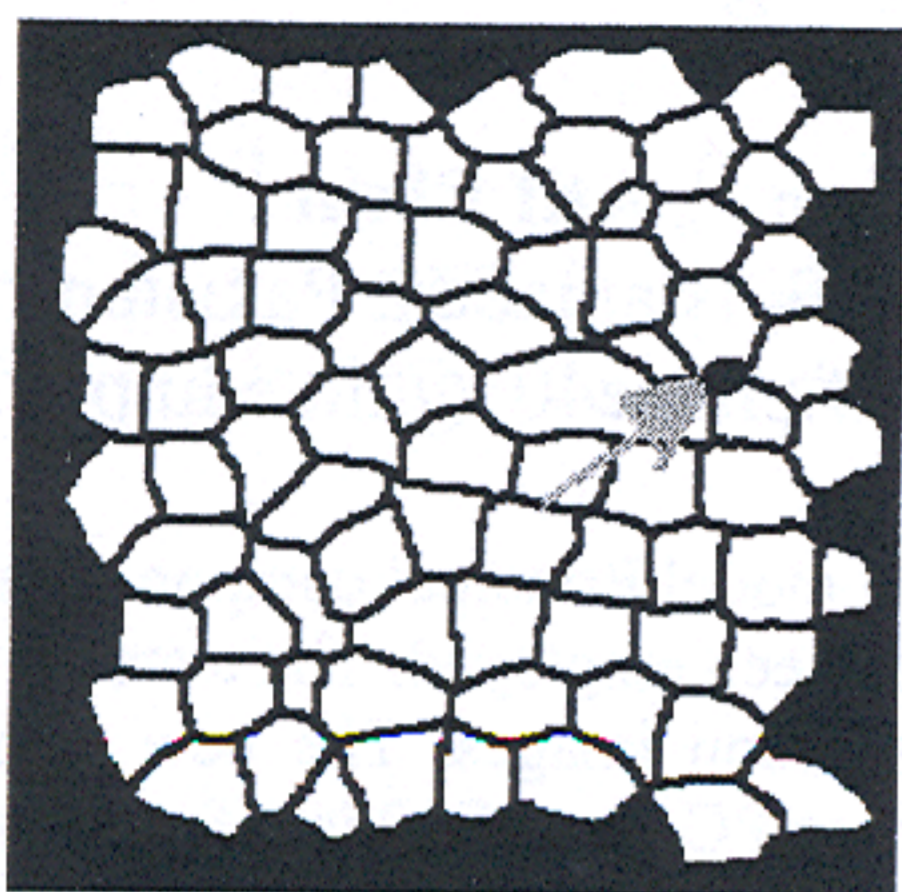


Fig. 11 – The image with a deleted small object

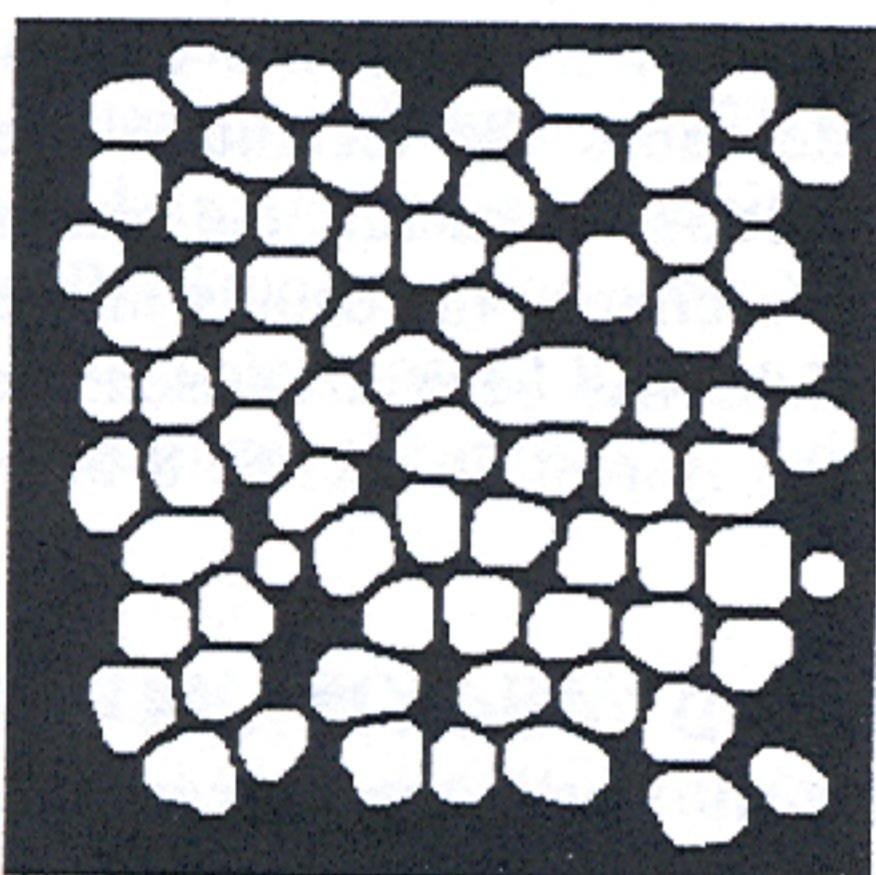


Fig. 12 – Correction of form of objects

## 5. CONCLUSION

In the paper, the scheme of computational experiments, methods of constructing finite element models of nano-samples of their AFM images, setting rules of the boundary conditions for simulation of contact interaction have been proposed. The results of computational experiments to determine the characteristics of contact interaction by means of the package LS-DYNA were presented. The obtained results show that it is possible to extract images objects and calculate the series of geometric and brightness characteristics and image features in such complicated images as nano-structures.

## 6. REFERENCES

- [1] Sellmyer, D. *Advanced Magnetic Nanostructures* / D. Sellmyer, R. Skomski. – Springer, 2006. – 514 p.
- [2] Szmaja, W. “Digital Image Processing System for Magnetic Domain Observation in SEM”// W. Szmaja // *J. Magnetism Magnetic Mater.* – 1998. – No. 189(3). – 353-365 p.
- [3] M. Yukio, I. Hisafumi, and K. Hitoshi, “Automatic Visual Inspection System for Thin Film Magnetic Head Wafer Using Optical Enhancement and Image Processing Technique,” in *Proc. SPIE Applications of Digital Image Processing XV*, Ed. by A. G. Tescher (SPIE Homepage) 1771, 20 (1993).
- [4] Q. Zhu, X. Wang, X. Zou, et al., “Feature Extraction for Magnetic Domain Images of Magneto-Optical Recording Films Using Gradient Feature Segmentation,” *J. Magnetism Magnetic Mater.* 248(2), 292 (2002).
- [5] L. Wang, Z. Fan, and D. E. Laughlin, “Trace Analysis for Magnetic Domain Images of L10 Polywinted Structures,” *Scripta Materiala* 47(11), 781 (2002).
- [6] P. Paturi, Larsen B. Hvolbaek, B. Jacobsen, and N. Andersen, “Image Correction in Magneto-Optical Microscopy,” *Rev. Sci. Instr.* 74(6), 2999 (1990).
- [7] A. Nedzved, S. Ablameyko, M. Tekielak, et al., Processing of Needkes-Like Images of Magnetic Domain Structures in Ultrathin Cobalt Wedge, 8th International Conf. on Pattern Recognition and Information Processing (PRIP'2005), May 18–20, 2005, Belarus, Minsk (2005), pp. 108–111.
- [8] Nedzved A., Dobrogowski W., Ablameyko S., Tekielak M. and Maziewski A. Analysis of nanostructures by magneto-optical images // *Pattern Recognition and Image Analysis*, Vol. 19, N.2, 2009, P. 321-333